ROBUST CONTROL DESIGN METHODOLGY FOR THE 6DOF FLIGHT-FORMATION OF PROBA-3

Joost Veenman, Daniel Serrano Lombillo, Raul Sánchez Maestro

SENER Ingeniería y Sistemas, S.A. Severo Ochoa, 4 (P.T.M.) 28760 Tres Cantos – Madrid (Spain), info@sener.es

ABSTRACT

PROBA-3 is one of ESA's technology demonstrators, which consists of two spacecraft flying in close formation in a highly elliptic orbit. Its aim is to create a Sun coronagraph instrument with the optical payload and the external occulter disc mounted on different spacecraft. One of its main challenges is to develop the GNC that maintains a flight-formation during the apogee arc with very stringent attitude and relative position requirements. The flight-formation consists of aligning both spacecraft with the Sun vector, while maintaining a fixed distance with sub-millimetre precision. In addition, various technology demonstration manoeuvres will be performed for virtual structure simulation (rotating the formation, while maintaining a fixed distance), and virtual telescope focusing (resizing the formation, while keeping the Sun vector aligned).

The control problem has been posed as a coupled 6 degree-of-freedom (6DoF) multi-input multi-output (MIMO) design task, which simultaneously takes care of both the attitude and the position. To meet the design specifications, modern H_∞- and μ-synthesis techniques have been utilised to obtain a robust controller. In addition, in-house developed simulation tools have been employed for validation purposes in a non-linear environment.

In this paper the step-by-step design techniques and accompanying tools used by SENER are presented, starting with the formulation of the control problem, working towards the justification of the designed controller, and resulting in a fully validated product both in frequency and time domain for integration with the full PROBA-3 system.

1. INTRODUCTION

PROBA (Project for On-Board Autonomy) is a programme developed by ESA for in-orbit demonstration of platform and payload technologies. Up to now, three missions have flown in this framework: PROBAs 1, 2 and V launched on 2001, 2009 and 2013 respectively. PROBA-3 is the continuation of these works in which precise formation flying technologies are to be tested. The reader is referred to [9] and [10] for some initial reporting. To this end, PROBA-3 builds on the knowledge acquired in previous PROBA projects, while further developing technologies for future applications. The project's prime contractor is SENER. In addition to this work, SENER will also produce the Formation Flying (FF) control which will manage the relative positioning and pointing of the spacecraft.

Typical Attitude and Orbit Control System (AOCS) design approaches require a certain pointing performance in order to obtain a certain scientific return. Positioning requirements generally become more lax, being constrained to absolute orbit control, and are generally independent of spacecraft attitude. The particularity for the PROBA-3 GNC is that spacecraft relative pointing and positioning requirements are both equally demanding in order to obtain a given formation such that attitude and position errors become dynamically coupled. This calls for a 6DoF controller development in which all of the contributors are tackled jointly.

One of the most well-known frameworks suitable for such a design task is called the H_∞/μ-approach [1], [2], [3], [4], [5], [6]. This framework consists of very effective synthesis and analysis tools that enable to:

- design H_∞-controllers (i.e. MIMO controllers with stability and performance guarantees),
- perform μ-analysis (i.e. robust stability and performance analysis for systems with structured dynamic and parametric uncertainties),
- synthesise robust controllers (i.e. design a robust controller by combining the previous two methods.

In particular these tools have been utilised to obtain a robust controller for the flight-formation stage.

The main goal of this paper is to present the control design methodology focusing on the workflow followed from requirement analysis to the production of a validated controller. In addition, the paper will outline the main mission and system aspects on which the formation flying control depends. Finally, a brief summary of the final verification approach is also provided.

2. MISSION DESCRIPTION

PROBA-3 mission consists of two spacecraft which will fly in high precision formation around a highly elliptical Earth orbit. As in previous PROBA projects, additionally to the technology demonstration mission, a scientific payload is included. The aim of this payload will be to make use of the flight-formation to form a large coronagraph capable of producing a nearly perfect eclipse allowing to observe the sun corona closer to the rim than ever before. The system is divided between both spacecraft such that one carries the optical head (Coronagraph Spacecraft or CSC) and the other the Occulter disk (Occulter Spacecraft or OSC). When

performing coronography, both spacecraft will keep a fixed inter-satellite distance of approximately 150 m. Figure 1 shows an artistic representation of the spacecraft.

Figure 1: PROBA-3 spacecraft artistic view

In order to have the OSC perform adequately, the spacecraft platform is designed to remain 'hidden' behind the occulter disk so that no additional shadow is cast.

In addition to the scientific goals, PROBA-3 also includes a set of formation flying in-orbit validation experiments with applications for future formation-flying missions. The aim is to validate the technologies necessary to have separate satellites maintain a desired geometry to achieve the function of a single large virtual spacecraft. The flight formation will exploit basic configurations: "rigid" long baseline instruments, synthetic aperture and separation of primary and secondary on a telescope. The manoeuvres to be tested will include:

- Formation retargeting: In this case, the formation will rotate itself as if it were a single rigid structure to achieve a different pointing configuration. Relative position and attitude requirements will be met throughout the whole manoeuvring phase.
- Formation resizing: The formation will modify its inter-satellite distances ranging from 25 m to 250 m, as in the case of a telescope focusing operation.
- Formation roll: For this manoeuvre, the formation will roll around the line defined by both payload elements.

In all formation flying manoeuvres, it will be the OSC who will be in charge of controlling the relative position. This means that the CSC position will be left uncontrolled while the OSC follows the desired relative trajectory.

Finally, PROBA-3 will also perform a Relative Dynamics Experiment aimed at testing technologies related to Active Debris Removal. The OSC will carry a Visual Based Sensor which will be used to approach an inert CSC in a non-cooperative experiment.

2.1. Orbit characteristics and derived requirements

The ideal orbit to achieve the best performance for a mission such as PROBA-3 would be an orbit around L-2. However, the high energy requirements for such an orbit have caused the mission to be designed around a different architecture. Indeed, both spacecraft are launched together and injected in a stacked configuration in their final operational orbit. This orbit is highly elliptical, with perigee and apogee altitudes of approximately 600 km and 60,000 km respectively, leading to an orbital period of about 19.5 h.

For such an orbit, the relative dynamics of the spacecraft, if left on free-fall, will be radically different in each phase of the orbit. During perigee the relative speeds will be much larger if compared to the apogee phase. For this reason, the mission has been designed such that formation flying technologies are only tested during 6 hours around the apogee arc. This allows to minimise the required propellant consumption to achieve the necessary forced motion. To this end, the main driver for the formation flying control sizing is the gravity gradient defined by the two slightly different orbits followed by each spacecraft.

After the end of the apogee flight, a two-point manoeuvre is computed and executed in order to brake formation, guarantee safe perigee passage in free drift, and reacquire formation at the beginning of the following apogee arc.

Figure 2 shows a schematic of this process: During the apogee, the orbit followed is defined by the CSC (the brown figure) while the OSC (blue disk) is in forced motion; whereas during the apogee, it is the OSC who defines the orbit and the CSC who manoeuvres with respect to it.

The gravity gradient force which, needs to be compensated by the position controller, becomes larger the further away one moves from the apogee. Since no orbit control is foreseen for PROBA-3, aerodynamic friction during perigee passages will constantly lower the orbital apogee. This means that the controller needs to be sized to compensate for gravity gradients ranging from the one in apogee at beginning of life to the one in the extremes of the apogee arc at the end-of-life orbit.

2.2. Performance indices and requirements

The performance of the formation can be quantified with respect to the relative position and attitude of both elements of the payload. The Coronagraph Instrument boresight axis will define the target line in which the OSC will try to position the centre of the Occulter disk. Besides, both spacecraft will control their attitude with respect to the Sun.

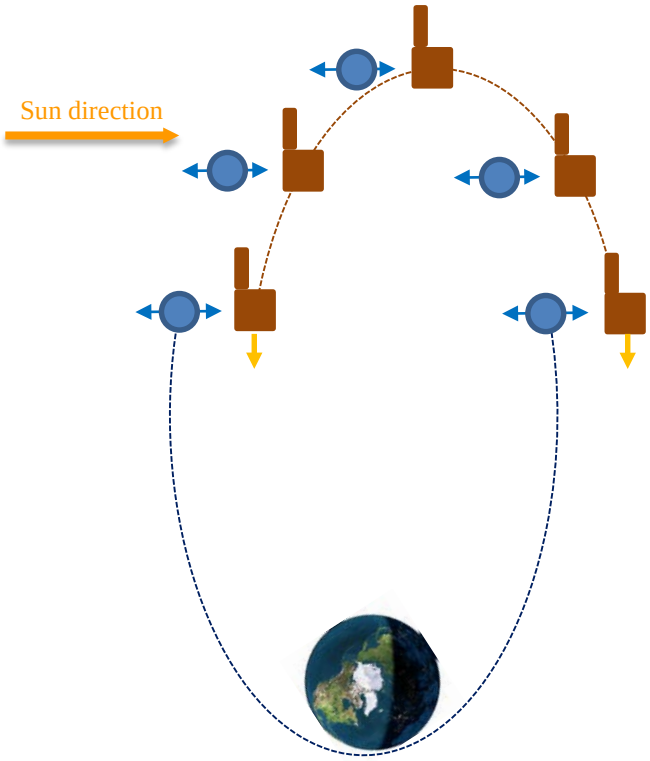

Figure 2: Relative position during apogee

For coronography, the most relevant performance index will be the relative position of the disk with respect to the Coronagraph Instrument boresight axis. This index leads to a combination of two very stringent requirements: The CSC pointing with respect to the Sun; and the OSC positioning with respect to the CSC. Other relevant performance indices include: CSC pointing stability to minimise image blurring; and OSC disk tilt to minimise stray light contamination and shadow geometry distortion. The following table summarises the latter objectives to be achieved by the formation:

Index		Value	Units
CSC absolute pointing error		7.07	arcsec
CSC absolute pointing stability		2.65	arcsec
OSC absolute pointing error		90	arcsec
Relative displacement error	@ 25 m	2.25	mm
	@ 150 m	4.88	mm
	@ 250 m	8.13	mm

Table 1: Performance requirements

Except for the Relative Dynamics Experiments (which will benefit of the changing relative dynamics throughout the whole orbit to control relative position) all the technology experiments will take place exclusively during the apogee arc. It is during this phase that the high accuracy relative metrology will be used. After formation braking, both spacecraft remain in Sun pointing without controlling the relative attitude. During the lower part of the perigee phase, a dedicated algorithm combines the GPS information from both spacecraft to accurately estimate the relative state. Once the GPS signal is lost (due to high altitudes), both spacecraft remain in free drift until the beginning of the next apogee arc, when the relative navigation function uses the propagated solution available to acquire the relative metrology. A proper estimation of the disturbing forces during the phase without relative metrology is necessary to achieve this acquisition. The main perturbation to be estimated here is the solar radiation pressure.

3. HARDWARE & GNC EQUIPMENT

In order to be able to meet the requirements, a dedicated set of metrology sensors and actuators is required. A High Accuracy Metrology system is being developed to measure relative position with sufficient accuracy. Additionally, off-the-shelf equipment is being used to complete the necessary GNC hardware suite. Table 2 summarises the units' description.

Unit	CSC	OSC
Relative metrology		
Fine lateral and longitudinal	Retro Reflector	Sensor & laser emitter
Coarse lateral	Sensor & laser emitter	Retro Reflector
Visual based	Mire pattern	Wide and narrow head units
GPS	2x receivers	
Payload		
Coronagraph Instrument	Optical head	Occulter disk
Shadow position sensor	Photodiodes	
GNC suite		
Star tracker	3x head units	
Inertial reference unit	8x accelerometers & 4x gyros	
Sun sensor	1 FSS & 3 CSS	
Reaction wheel	4 unit pyramid	
Propulsion	8x hydrazine thrusters	12x cold gas thrusters

Table 2: Hardware & units

Since both Spacecraft carry components of the metrology system, an inter-satellite radio frequency link has been implemented to allow for inter-spacecraft communication. When in formation, the CSC will send its sensors' data to the OSC and the OSC will have the ability to command the CSC.

From a structural point of view, a very accurate knowledge of the relative positioning and alignment of the GNC units and the payload is required in flight. To achieve this, both spacecraft carry an Optical Bench Assembly (OBA) where the units are mounted. This bench has been developed to thermally and mechanically isolate the units from the rest of the spacecraft and maximise structural stability in flight.

3.1. FLLS & derived requirements

The highest accuracy metrology available is the Fine Lateral and Longitudinal Sensor (FLLS). This unit is based on a collimated laser beam emitter on the OSC and a retro-reflector on the CSC. This laser beam has a radius of 20 mm, requiring itself a high pointing accuracy to have the retroreflector in the field of view at 150m.

During earlier phases of design, the intention was to have the FLLS mounted on the CSC as close as possible to the payload. However, it was found that the misalignments and deformations suffered after launch could cause a de-pointing large enough to make it impossible to have the retro-reflector on the OSC fall within the FLLS field of view. It was then decided to change the mission architecture and accommodate the unit on the OSC. This allows for any misalignments to be compensated for in flight and enables to adequately point the FLLS boresight towards the retro-reflector at the same time that the occulter disk centre is positioned over the target line. Figure 1 sketches the main idea.

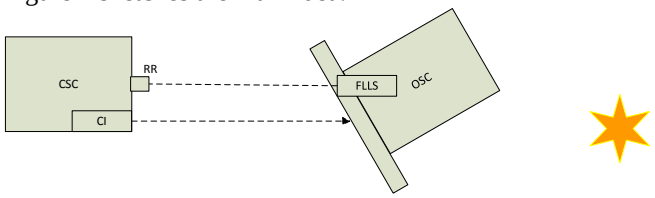

Figure 3: FLLS on OSC configuration

This new configuration, which is needed due to the system limitations, has had a great impact on the OSC controller design. Due to the limited FLLS field of view, the OSC attitude controller needs to have an accuracy in the order of magnitude of few arcseconds to guarantee that the FLLS metrology is not lost. This becomes particularly challenging since it needs to be achieved at the same time as the stringent relative positioning requirements, i.e. while the OSC propulsion system is being actuated, which introduces significant perturbing torques.

3.2. Need for handover and coarse metrology

After the perigee passage, relative metrology needs to be re-acquired. However, the achievable accuracy in the execution of the two-point manoeuvre plus the errors in the estimation of the relative state make it necessary to have an intermediate coarse metrology to hand over to FLLS. For this purpose, both the visual based sensor and the coarse lateral sensor can be used. From control perspective, this means that, when beginning the forced motion phase, the system will start with relatively large position and speed errors and will need to converge to accurate ones to begin the scientific operations. Because of this, a two-mode controller is considered. Both controllers will be 6DoF, but the first needs to be capable of correcting the initial state as fast as possible, whereas the second need to produce the best possible performance during operations. The transition between both controllers is currently being studied to guarantee best possible performance.

3.3. Actuators

Attitude control on OSC does not have large torque perturbations to compensate for, which should lead to small inertia reaction wheels. However, in order to optimise the system design, the decision has been made to carry the same reaction wheels on both spacecraft. On the other hand, due to its asymmetrical nature, the CSC does have to compensate for a noticeable solar radiation pressure torque. In addition, it needs to be able to store the angular momentum built up from this torque. This has been the sizing factor for the reaction wheels, which has caused the reaction wheels' noise to be a significant torque perturbation for the attitude controller.

The CSC carries 1 N hydrazine thrusters which are only used for the formation acquisition and braking manoeuvres, given their high thrust level as compared to the position controller requirements.

The OSC controls the relative position with a set of 10 mN cold gas thrusters. The layout has been designed to be able to produce pure forces and torques around all axes as illustrated on Figure 4. However, actuator management is performed such that only forces are executed with thrusters and torques with reaction wheels. Additionally, forces are commanded sequentially along each axis, instead of all at the same time. The reason for this is to minimise undesired torque perturbations due to the minimum opening time of the thrusters. By doing so, one can guarantee that commanded opening times will be equal for symmetric thrusters. If thrust was commanded along all axes at the same time, this would lead to non-symmetric opening time commands, which could result in thrusters being commanded below their minimum opening time, leading to undesired torques.

Due to the fact that relative position will be controlled very accurately during at least 6 hours per orbit, the number of thruster firings throughout the whole mission lifetime could result too large. This parameter needs to be minimised to avoid thruster malfunctioning. For this reason, control commands are pulse width modulated with a period of 10s. This introduces a non-linearity in the system which will force the control bandwidth to be far away from this period.

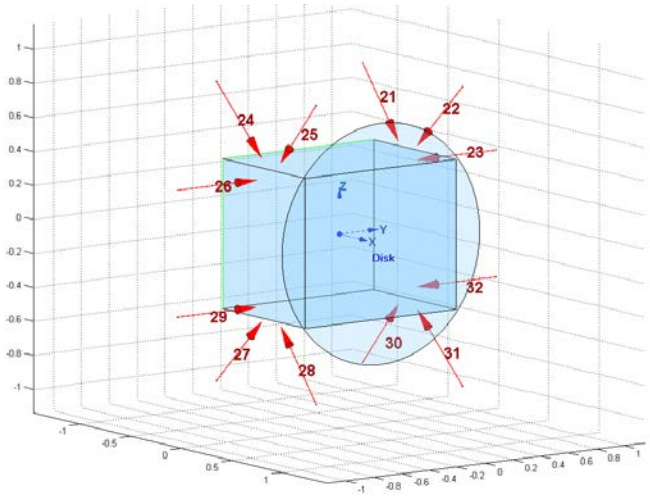

Figure 4: OSC thruster layout

4. THE HIGH PRECISION FLIGHT FORMATION CONTROL PROBLEM

The FF- and the SC-GNC systems have the demanding task of maintaining the flight-formation in a relative position and attitude with a very high accuracy, precisely as described in Section 3.

To do so, the guidance module provides the desired position and attitude profiles. Subsequently, these are compared with the real position and attitude trajectories, which are retrieved from the navigation system. Roughly speaking, the controller is then supposed to minimise the differences between the desired and the actual relative positions and attitudes.

To maximise the system's performance, the controller not only consists of a feedback unit, but also a feedforward compensator. Given an estimate of the gravity gradient, the guidance function computes the ideal actuator commands that are needed to follow the given guidance profiles. In addition, the feedback controller simultaneously corrects the remaining tracking errors that are e.g. caused by external disturbances and model mismatches. Note that the control function is designed such that the feedback controller achieves the design specifications without the feed-forward contribution. The feedforward compensator is, hence, only used to further optimise performance.

For the FF-GNC system, the most demanding manoeuvers are the ones during the experiments, when the high precision metrology is operating. Throughout these manoeuvers only one spacecraft (i.e. the OSC) is subject to position control, while, for obvious reason, both spacecraft need to be actively controlled to maintain their desired attitudes.

One of the goals of the mission is to design a robust multi-input multi-output (MIMO) 6 degrees-of-freedom (6DoF) feedback controller through the use of modern robust controller design techniques such as e.g. H_∞- and μ-synthesis [1], [2], [3]. Although the corresponding theory has matured over the course of the last three decades, its application remained rather challenging for several reasons:

- Its application requires a thorough understanding of the theory behind the tools.
- To apply the techniques, one needs to translate the given design specifications into corresponding frequency dependent weighting functions, which is nontrivial.
- Because the dimension and the complexity of the involved models are typically rather high, the tools are pushed to their limits from a computational point-of-view.
- The obtained controllers are typically of high order, which makes them unsuitable for practical use. Hence, it requires model reduction techniques to facilitate the implementation.

Nevertheless, despite these and various other reasons, the tools are very systematic and go far beyond the possibilities that one would have with classical design techniques. In the following section we will discuss in more detail how the tools can be applied.

5. CONTROL DESIGN METHODOLOGY

To design a robust controller that meets all the design requirements, it is essential to systematically carry out a predefined protocol. This section presents the step-by-step procedure that has been followed to obtain the desired results. The essential features of the approach are shown in Figure 5. An illustrative sketch of the design results of the high precision control will be presented along the way. Here we note that these are preliminary results that are subject to change.

5.1. Modelling

Since the H_∞- and μ-synthesis tools are model based control algorithms, it is essential obtain a representative model that is suitable for synthesis: i.e. a linear, time-invariant model that admits a state-space realization. Such models can be obtained from a (nonlinear) Simulink model by linearizing about a certain operation point along the trajectory that is to be followed, or, simply, by manually deriving the equations of motion.

For the PROBA-3 mission, we are also concerned with uncertainties. For this reason, it is much less cumbersome to choose the manual derivation of the equations-of-motion for both the relative orbital position and attitude dynamics of the OSC as well as the coupling effects between them. This also allows to directly define the systems' parameters as

uncertainties such as e.g. mass, moment of inertia, centre-of-mass, etc.

In particular, since the OSC is subject to a forced motion and the CSC is freely floating in a highly elliptical orbit, an uncertain non-linear dynamical model has been formulated which describes the coupled motion of the relative orbital position of the OSC with respect to the CSC and the attitude of the OSC. This model was linearized about a carefully chosen presumed worst-case orbital rate in the apogee phase, where the actual fine control takes place. This yielded a linear time-invariant uncertainty model that is suitable for robust synthesis. By setting the uncertainties to their nominal value, one subsequently obtains a model that is valid for nominal synthesis.

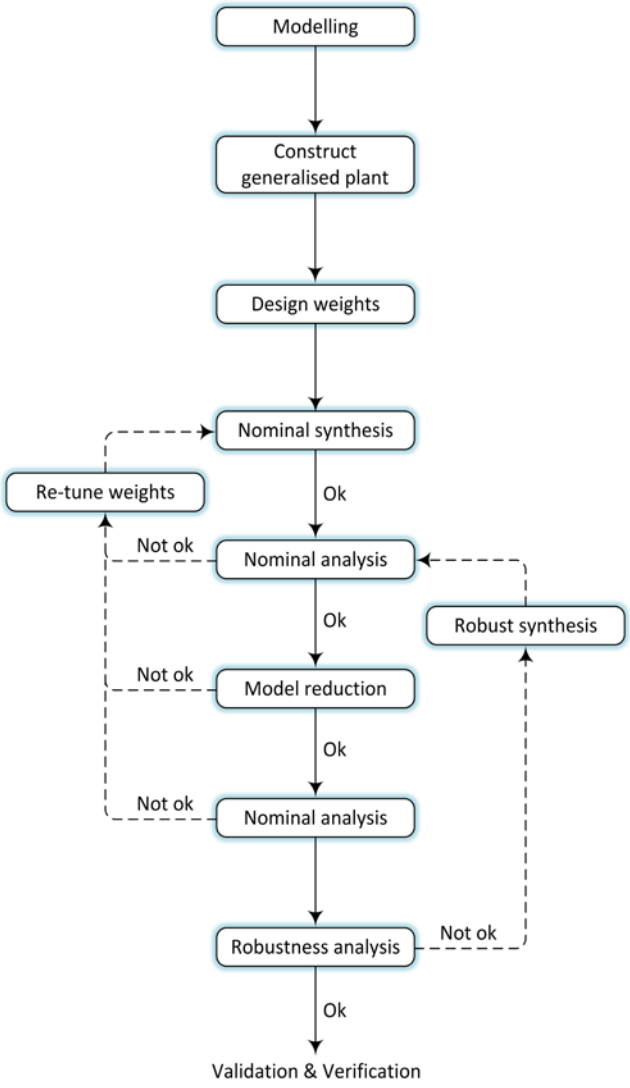

Figure 5: Control design methodology

5.2. Generalised plant

To apply the H_∞- and μ-synthesis approach, it is necessary to formulate a so-called generalised plant. Roughly speaking, this defines the feedback interconnection of the uncertain plant model $G(\Delta)$ with the to-be-designed controller K. Here the notation $G(\Delta)$ is used to denote that the plant G depends on a collection of uncertainties Δ. A schematic representation is given in Figure 6.

As can be seen, the interconnection describes a feedback loop with reference input r, disturbance input d and measurement noise input n, which are self-explaining. In addition, there are performance outputs e_1, e_2 and e_3, which represent the tracking error output, the control output and the plant output respectively. Finally, the blocks $-I$, L and L_c are auxiliary scaling and commuting blocks, which are of minor importance from a conceptual point of view.

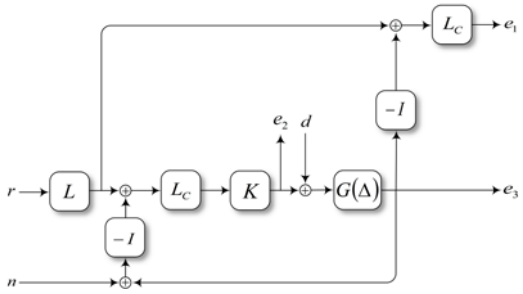

Figure 6: Generalised plant

The choice of this particular interconnection (note that there are many other possibilities) is motivated by the fact that we need to design a controller K that, for all modelled uncertainties:

- guarantees stability of the system interconnection,
- minimises the H_∞-norm from the inputs r, d and n to the performance outputs e_1, e_2 and e_3.

The latter means that K needs to ensure that the tracking error e_1, the control effort e_2 and the plant output e_3 all remain within their given bounds for some given reference trajectory r and despite the presence of uncertainties, external disturbances and measurement noise.

5.3. Designing weights

It is essential to emphasise that direct minimisation of the H_∞-norm from the inputs the r, d and n to the outputs e_1, e_2 and e_3 would not yield any meaningful result.

To achieve the desired design specifications, it is necessary to shape the frequency spectrum of each in- and output through the use of frequency dependent weighting functions. This is done by extending the feedback interconnection of Figure 6 as shown in Figure 7. Here the

output signals z_1, z_2 and z_3 are the filtered versions of e_1, e_2 and e_3, while r, d and n are filtered versions of w_r, w_d and w_n.

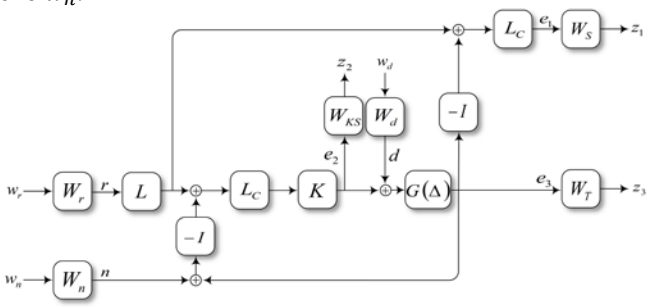

Figure 7: Weighted generalised plant

Typically, the input weights W_r, W_d and W_n are used to capture the knowledge that one has about the signals r, d and n:

- Reference trajectories are often designed as smooth signals to avoid abrupt responses to e.g. sharp impulses and steps. In such a case, W_r can be chosen as a simple low-pass filter.
- The sources for external disturbances can be diverse. For example, once could think of solar pressure, thruster misalignments, micro-vibrations, sloshing effects, flexible modes, etc. Such disturbances can often be represented W_d in the form of low-, band, or high-pass filters.
- Typically, measurement are disrupted by e.g. noise or sinusoidal disturbances. In this case, W_n can be used to describe the spectrum of the noise.

On the other hand, the performance weights W_S, W_{KS} and W_T are used to shape the sensitivity, complementary sensitivity and noise sensitivity functions S, T and KS respectively. Among other purposes,

- W_S is typically used to guarantee good tracking at low frequencies,
- W_{KS} is often used to penalise control at high frequencies,
- W_T can be used to constrain the maximum bandwidth of the controller.

We emphasise that the latter description only serves as a brief illustration of the possibilities. It is outside the scope of this paper to discuss any further details.

5.4. Nominal synthesis

Given the generalised plant and the weighting functions, it is now possible perform a nominal controller synthesis. This is done by setting the uncertainties to their nominal values, which yields the nominal weighted generalised plant. Subsequently, it is possible to employ the H_∞- design tools that are available within the robust control toolbox of MATLAB [4], [5].

For the fine control problem we found a feasible solution which guaranteed the H_∞-norm of the weighted closed-loop system to be sufficiently small.

5.5. Analysis

To validate whether or not the designed controller meets the design specifications, one typically starts with an initial analysis. Among others, this includes a validation through sigma plots (i.e. a plots of the maximum singular values of the frequency response of a system) as well as time-domain simulations with a low or medium fidelity Simulink model. For further details on the control verification environments we refer the reader to Section 6.1.

To avoid a full presentation of the preliminary results, we have plotted the maximum singular values of position part of the sensitivity function S (i.e. the map from the reference input r to the postion part of the performance output z_1) versus the inverse of the position sensitivity weight W_S. The results are shown in Figure 8. As can be seen, the sensitivity function (the blue dashed line), lies entirely below the inverse of $W_S^{-1}(pos)$, which indicates good tracking at low frequency up to about 0.01 rad/sec and with a steady state error of about -120 dB. As indicated by the grey box, the nominal requirements are clearly met.

To give a sketch of the nominal time domain simulations results, we have plotted various the OSC's attitude responses caused by nonzero initial positions of 2.5 cm in a random direction. The responses are shown in Figure 9. Also here the responses remain within the given limits as indicated by the dashed lines. Note that these values are still subject to change and that such nonzero initial conditions are rather non-realistic.

We emphasise that the simulations have been obtained without the use of a feedforward controller. Hence, in reality the responses would be much better. Further note that a thorough analysis would include also other sigma plots for various mappings that can be deduced from Figure 7 and Figure 8. In addition, a typical analysis would include, for example, Nichols plots and other time domain simulation results.

5.6. Model reduction

As one of the main drawbacks of the H_∞- approach, the tools yield unstructured controllers that have the same number of states as the weighted open-loop generalised plant. In our case, this was 48 states.

Evidently, such a controller would not be suitable for implementation directly. Fortunately, there are dedicated tools that enable the designer to reduce the state dimension of

the controller drastically. The most of the well-known techniques is called balanced truncation, which allowed to reduce the state-dimension with 27 to 21.

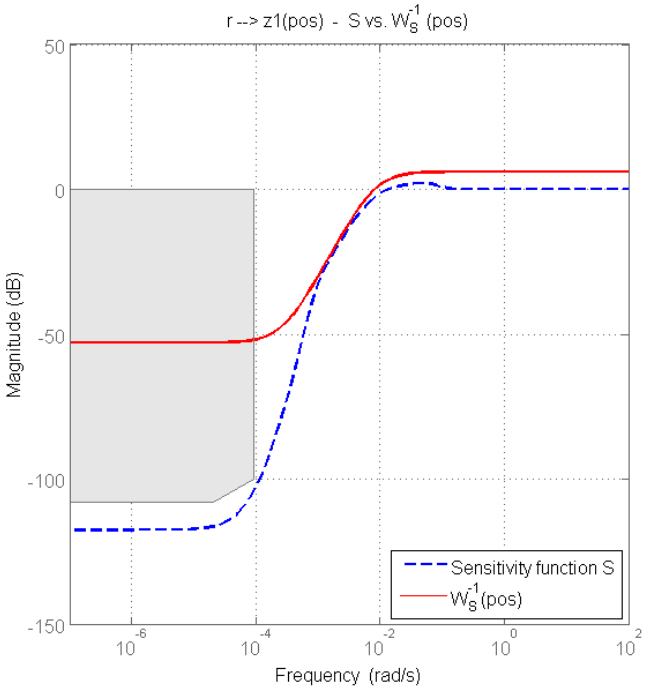

Figure 8: Position sigma plot of the sensitivity function S versus the inverse of the weighting function W_S

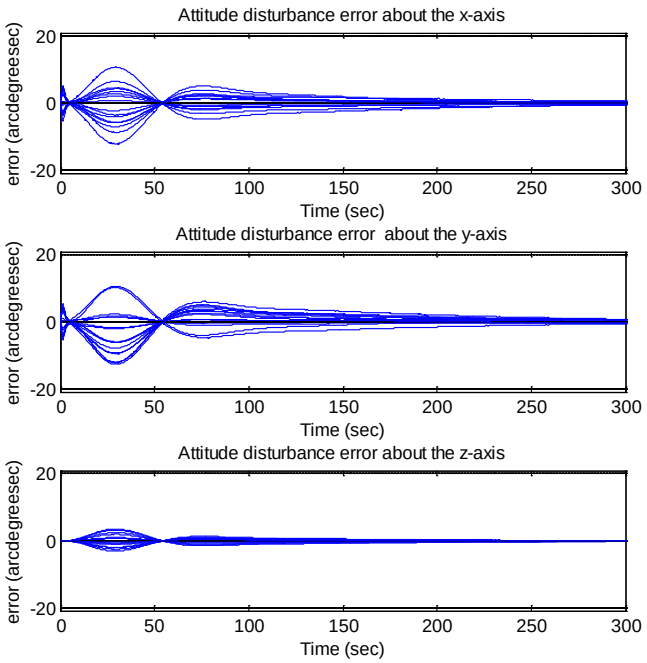

Figure 9: Time simulations of the nominal controller in the absence of uncertainties.

After having performed the model reduction step, it is essential to repeat the previous analysis step in order to see if and by how much the controller's performance has degraded. If too much, either the model reduction step has to be repeated, or one has to re-tune the weighing functions and perform a new synthesis as indicated in Figure 5.

5.7. Robustness analysis

In a next step, once the nominal controller is compliant with the nominal design specifications, it is of paramount importance to validate the system's performance in the presence of uncertainties.

Indeed, although the nominal controller might perform well if the uncertainties are set to their nominal value, even small deviations might cause drastic performance degradations or jeopardise stability.

An important tool to access the robustness properties of an uncertain system is the so-called μ- or structured singular value approach [6]. Given an uncertain system the technique allows to compute the upper bounds of the worst-case stability and performance margins.

To apply the tools, it is necessary to reformulate the uncertainty model as a so-called linear fractional representation (LFR) (i.e. reformulate $G(\Delta)$ as $G(\Delta) = G_{11} + G_{12}\Delta(I - G_{22}\Delta)^{-1}G_{21}$). This limits the application of the tools to plants with a rational dependency on the uncertainties. In addition, the μ-tools are confined to consider linear time-invariant parametric and dynamic uncertainties. However, the latter restriction can be easily dropped if considering the more general framework of integral quadratic constraints [7], [8].

Since our model is compatible with the μ-tools, it is straightforward to obtain an LFR with the robust control toolbox of MATLAB by using commands like "ureal", "lft", "lftdata" etc. Among others, the PROBA-3 model consists of the following uncertain parameters: mass, moment-of-inertia, centre-of-mass (COM), measurement delay, etc.

If the robustness analysis confirms that the controller is robust against all of the modelled uncertainties, the controller has passed all control design steps. Further analysis are subsequently to be performed in the validation and verification process. On the other hand, as illustrated in Figure 5, if the robustness analysis indicated large performance degradations due one or more uncertainties, the nominal design has to be robustified as will be discussed in the following subsection.

To illustrate the main idea, Figure 10 shows:

- the sigma plots of the nominal weighted closed-loop plant in accordance with Figure 7.
- the sigma plots of the uncertain weighted closed-loop plant for a random set of COM deviations with a maximum radius of 5 cm.

- an upper bound of the worst-case structured singular value (i.e. μ).

As can be seen, performance degrades drastically in the presence of centre-of-mass uncertainties. This is confirmed by the time-simulations as shown in Figure 11.

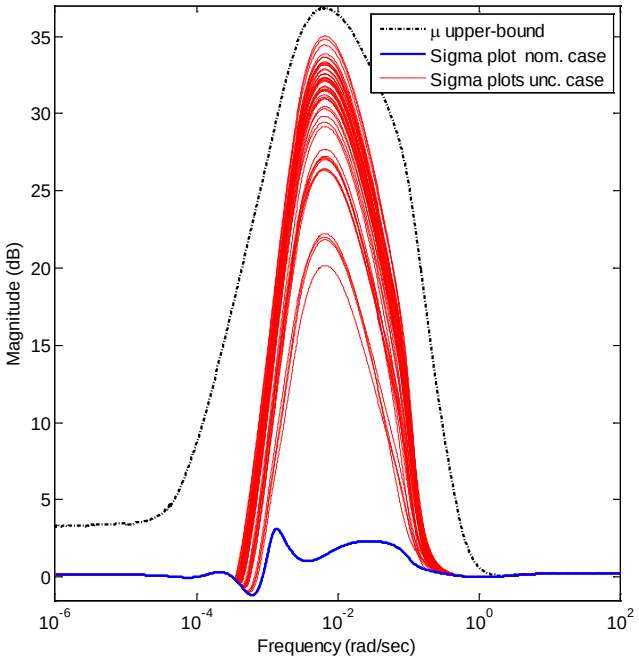

Figure 10: μ - analysis for the nominal controller with centre-of-mass uncertainties

5.8. Robust synthesis

If the nominal controller is not robust to all modelled uncertainties, the controller needs to undergo a robustification process, something which can be done with the μ-synthesis tools. Given the weighted open-loop generalised plant this boils down to running the command "dksyn", which is a powerful algorithm for obtaining robust controllers.

In the particular case of the fine control of PROBA-3, we have robustified the nominal controller against COM uncertainties (and others, which are not discussed) by employing the μ - synthesis algorithm.

As a final result, the previous analysis have been repeated for the obtained robustified controller. As can be seen in Figure 12 and Figure 13, both the worst-case gain as well as the time domain simulations have improved significantly. In addition, further analysis confirmed that the robustified controller is also robust against all other modelled uncertainties.

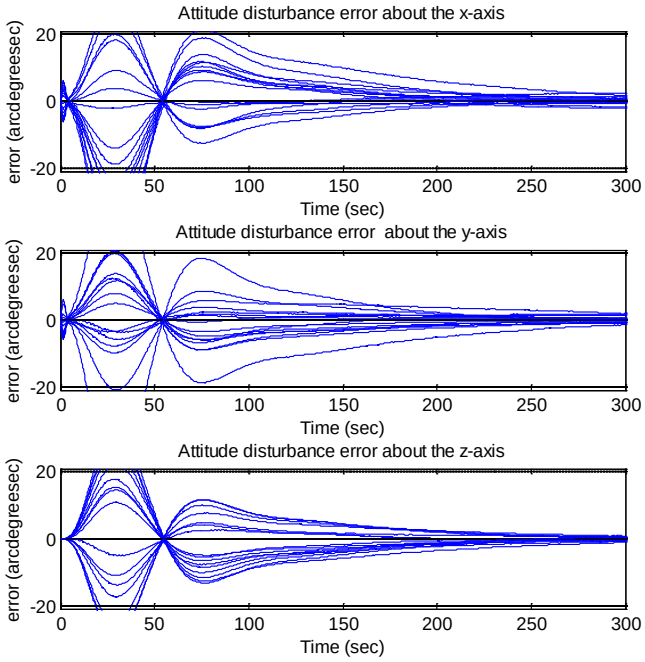

Figure 11: Time simulations of the nominal controller in the presence of uncertainties.

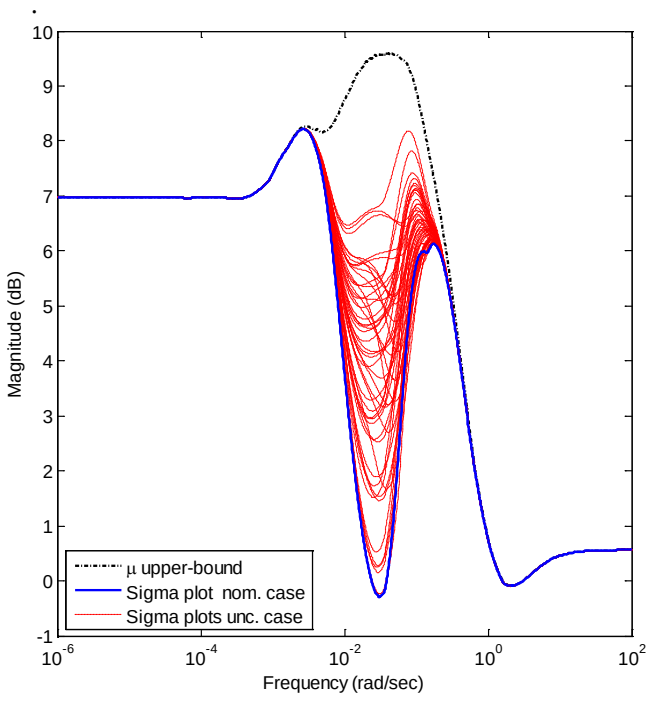

Figure 12: μ - analysis for the robust controller with centre-of-mass uncertainties

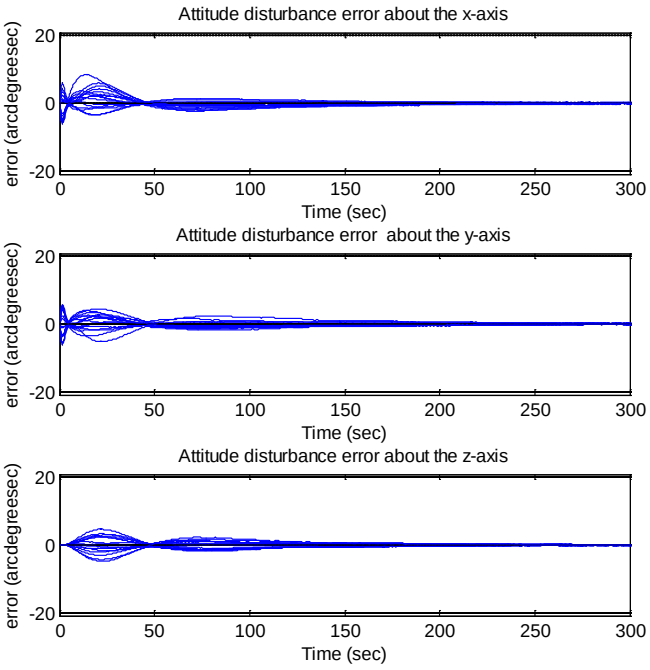

Figure 13: Time simulations of the robust controller in the presence of uncertainties.

6. VERIFICATION ENVIRONMENTS

Requirements are flown down from system level to control function design. From the high level system requirements, a subset is derived for the formation flying subsystem. From the point of view of performance indices, in order to meet system requirements, all mechanical, structural and thermal contributors need to be accounted for before allocating the FF-GNC performance requirements. From these, a second flow down is done for control function level. Errors derived from GNC units and navigation accuracy need to be accounted for before allocating control performance requirements.

6.1. Control verification: SENERIC

The control function is then designed (see **Section 5**) to meet its performance requirements. At this level, a time domain simulator is implemented which is used for design purposes as well as to verify lowest level requirements. This simulator is based on SENERIC, an internal tool developed by SENER for AOCS development and verification. In this tool, the emphasis has been put on the development of an extensive library of simulation models within the MATLAB/Simulink environment. These models range from dynamics and environmental models to AOCS hardware models to complete closed loop simulators. However, visualization, analysis and post-processing tools are also included.

In this environment, highly representative models of the thrusters and reaction wheels are implemented. Additionally to the controller, the actuator management function is also tested. Simplified sensor models as well as navigation and guidance modules are included to close the loop.

This environment is designed to include representative models for control verification, but to minimise to its minimum the complexity of the rest of the GNC or vehicle management. High fidelity environmental simulation is not desirable either. For example, since the controller will only be used during the apogee, full orbit simulation is not considered necessary.

Such an environment has the advantage of being extremely agile and versatile, so that as many simulations as are deemed necessary can be run in a short period of time, including batch parametric simulations such as Monte-Carlo runs.

The fact that the simulator already includes the GNC feedback loop with actuators, is extremely helpful for subsequent activities. The controller generated after this first phase of verification, will have already solved many of the problems which otherwise would only be discovered in the integration into more complex simulator environments.

6.2. FES

The Functional Engineering Simulator (FES) is where the full formation flying software will be tested at MATLAB/Simulink level. In this environment, the full high fidelity dynamic and kinematic environment is simulated. Sensors and actuator models are included with their real interfaces and the best knowledge available for their performance.

This environment is already valid for subsystem and system level requirement verification.

In the FES, both spacecraft are simulated. A layer of software is included as interface between the formation flying software and the units. This is representative of the real on-board software which will be present on the spacecraft computers.

The FES is also designed to support parametric batch simulations for statistical performance analysis.

In the PROBA-3 mission, automatic code generation of the formation flying software is foreseen. This code will be tested in the FES before integration into the following verification step.

This environment is already available for preliminary testing. However, it will be updated over the project lifetime to include the increasing level of understanding of unit characteristics.

The FES is being developed by GMV, with contributions from SENER and NGC Aerospace Ltd.

6.3. SBTB

The Software Based Test Bench will be the final step in the GNC verification. This environment will have a high fidelity simulation of the on-board computer and electrical interfaces. The full flight software will be tested in real time simulations. For this reason, batch 11 simulations are not foreseen for this environment.

The SBTB is being developed by Spacebel s.a.

7. CONCLUSIONS AND FUTURE ACTIVITIES

PROBA-3 is currently in the middle of the Phase C activities. Some preliminary design work has been carried out for the formation flying control in order to develop the necessary tools and methodologies for the final controller implementation. Results have been obtained using design criteria based on SENER engineering expertise. However, the requirement specification is not yet final, and a proper definition and quantification of uncertainties is still to be produced. The workflow described here will need to be repeated when the system's requirements from formation flying control are further defined.

Finally, formal verification of both subsystem and system requirements will be achieved by making use of the described testing environments.

REFERENCES

[1] J. Doyle, K. Glover, P. Khargonekar, and B. Francis, "State-space solutions to standard H_∞- and H_2-control problems," *IEEE Transactions on Automatic Control*, vol. 34, no. 8, pp. 831-847, 1989.

[2] P. Gahinet and P. Apkarian, "A linear matrix inequality approach to H_∞- control problems," *International Journal of Robust and Nonlinear Control*, vol. 4, no. 4, pp. 421-448, 1994.

[3] T. Iwasaki and R. Skelton, "All controllers for the general H_∞- control problem: LMI existence and state-space formulas," *Automatica*, vol. 30, no. 8, pp. 1307-1317, 1994

[4] G. Balas, R. Chiang, A. Packard, M. Safonov, "Robust Control Toolbox," *Tech. rep., The MathWorks Inc.* (2005-2008).

[5] R. Chiang and M. Safonov, "Robust control toolbox, ver. 2.0, Mathworks Inc. 1992.

[6] A. Packard and J. Doyle, "The complex structured singular value," *Automatica*, vol. 29, no. 1, pp 71-109, 1993.

[7] A. Megretski and A. Ranzer, "System analysis via integral quadratic constraints," *IEEE Transactions on Automatic Control*, vol. 42, no. 6, pp. 819-830, 1997.

[8] J. Veenman, C. W. Scherer, and H. Köroğlu, "Robust stability and performance analysis based on integral quadratic constraints," submitted for publication in *European Journal of Control*.

[9] L. Tarabini, *et al*, "PROBA-3 Formation Flying Demonstration Mission Design" *5th ICATT*, ESTEC, 2012

[10] R. Sánchez-Maestro, *et al*, "PROBA-3 High Precision Formation Flying Control System" *5th ICATT*, ESTEC, 2012.